Cell size and nucleo-cytoplasmic ratios of meibocytes in the anterior acini of the upper eyelid Meibomian glands in rabbits

Doughty, Michael J.

Published in:
Veterinary Ophthalmology

DOI:
10.1111/vop.12424

Publication date:
2017

Document Version
Author accepted manuscript

Cell size and nucleo-cytoplasmic ratios of meibocytes in the anterior acini of the upper eyelid Meibomian glands in rabbits

Michael J. Doughty, PhD

Sources of support: none.

The author has no commercial or proprietary interest in any concept or product discussed in this article.

Address communications to M. Doughty: Glasgow-Caledonian University, Department of Vision Sciences, Cowcaddens Road, Glasgow G4 OBA, Scotland.
Tel: 44-(0)141-331-3393; Fax: 44-(0)141-331-3387. E-mail address: m.doughty@gcal.ac.uk

ABSTRACT
Objective. To assess the morphological details of the acini of the normal Meibomian gland
Methods. From 6 young adult pigmented rabbits, the upper eyelid was prepared in extended configuration by glutaraldehyde fixation. Tissue block sections approximately 0.5 to 1 mm from the eyelid margin were assessed by light microscopy in sagittal sections and transmission electron microscopy (TEM) in coronal sections. TEM images at between 1000X to 2000 X magnification were enlarged onto A3-sized prints and cell size and nuclei measured by planimetry.
Results. LM sagittal sections revealed clusters of variable sized acini, sometimes appearing to be slightly overlapping and without any obvious spatial organization of the internal cells (meibocytes). The estimated areas of the acini were close to 6500 sq micron. Coronal sections, as examined by TEM, allowed for visualization of small to large acini (average diameter 82 +/- 17 microns, with an estimated area of 5500 sq. microns) containing variable numbers of immature (partly differentiated) or mature (fully-differentiated) meibocytes with a distinct spatial organization. The average area of the meibocytes was 158 +/- 81 square microns, and they usually appeared to have a single nucleus (with an average sectional area of 29 +/- 12 square microns). Within individual acini, peripherally-located immature meibocytes tended to be smaller and have higher nucleo-cytoplasmic area ratios, while more centrally mature located meibocytes tended to be slightly larger and had lower or much lower nucleocytoplasmic ratios.
Conclusion. Comparative studies on Meiboina glands can be undertaken with objective assessments to assess for normality or abnormality.

KEY WORDS rabbit, conjunctiva, eyelids, Meibomian glands, electron microscopy, morphometry, meibocytes, nucleo-cytoplasmic ratio

INTRODUCTION

The mammalian eyelids contain the gland of Meibom or Meibomian gland,[1-4] also referred to as the main tarsal glands.[2,4-6] Descriptive histology-based studies on domesticated animals, primates and humans indicate that the gland is composed of numerous secretory units opening onto narrow ducts (ductules), connected to a main outlet duct opening anterior to the ocular-mucocutaneous junction at the eyelid margin. This gross organization has almost invariably been visualized in suitable sagittal (histologic) sections (also referred to as longitudinal or transverse sections) through the eyelid. The secretory units that make up the actual glands have been referred to 'alveolae',[7,8] 'lobulated clumps',[9] (lobulated) acini,[10] 'lobules',[3] or as 'overlapping adenomores'(secretory units).[2] These alveolae and / or lobules are now generally referred to as acini, with perhaps numerous acinar units contributing to (multi)lobulated alveolae.

Overall, the histological appearance of these secretory units has been rather different and appears to depend on the exact location of the sections and their orientation with respect to the tarsal surface and / or the eyelid margin. When viewed at lower magnification, all that may be evident is the sub-capsular structure as slightly irregular outlines of these units loosely organized into discrete clumps or groups with little or no evidence of the inter-connecting ductile system.[5,6,11-16] The actual secretory nature is not evident in such clumps with the units seen to have a relatively amorphous content such that the individual cells (meibocytes) are not uniformly evident. In other sections, perhaps at slightly higher magnification, some meibocyte nuclei can be visiblet, [3,10,17-22] and just sometimes the individual meibocytes with their cell borders can be seen.[4,23-28] The cells seen, however, do not have any obvious organization and so better sectioning and viewing methods as well as objective assessments are needed to underpin histopathological diagnoses of gland dysfunction. This is especially needed because much of what has been written about the Meibomian glands appears to be derived from perspectives from other sebaceous (secretory) glands.

It has been stated, for example, that in the individual acini of the Meibomian glands there is an 'outer' or 'peripheral' layer of undifferentiated basal cells and that these progressively enlarge as they differentiate and fill with oil droplets.[10] Another report, this time on rat rather than human tissue, states that there is just a single layer of basal cells,[25] and that after injection of [3-H] thymidine this label was very quickly taken up by some of these basal cells. Over a few days labelled cells could be seen to towards the center of the acini, a migration that was considered to reflect mitoses and multiplication of the cells associated with differentiation of the acini. From studies on primate Meibomian glands, it was noted that the peripheral cells in the acini were smaller and had an elliptical-shaped nucleus while more centrally-located differentiated (mature) cells were larger and had a round nucleus,[23] and this perspective is also given, along with a schematic diagram with the nuclei having similar sizes.[10] It has, however, also been noted that in the largest hypermature meibocytes the cell nuclei change to a 'pyknotic' appearance,[4] perhaps with those cells with pyknotic nuclei being found close to the ductules of the gland.[23] This change could reflect the last aspect of the acinar function in that the contents change into the meibum secretion, a transformation referred to as 'degenerating cells',[24] 'decomposition',[25] or 'disintegration',[4,16] with it being implied that this process starts at the center of the acini.[23] In heavy metal-stained electron microscopy tissue sections, this transformed material can appear as an amorphous mass with no cellular detail remaining.[29]

Overall, the outcomes of the numerous histology studies have been largely qualitative and basic measurements of the individual acini (lobules) and their cells have not been reported upon, perhaps because of the rather variable appearance obtained in different sections. The goal of the present study was, therefore, to objectively investigate the fine structure and

ultrastructure of the acini of the rabbit Meibomian glands, particularly as viewed in coronal sections, to see how morphometry could be used to assess the differentiation (maturity index) of the meibocytes as well to assess whether or not there was a (discrete) sub-population of meibocytes with pyknotic nuclei.

MATERIALS and METHODS

Animals

The animal use protocol was in accord with the ARVO resolution on the Use of Animals in Research, was approved by a local animal care committee.[30-33] Female Dutch belt pigmented rabbits were obtained from a certified animal breeder, quarantined for 7 to 10 days prior to use to ensure there were no obvious signs of nasal or GI tract disease and eyes checked by slit-lamp examination. Over a 3 year period, six different animals aged 9 to 11 weeks (1.9 to 2.3 kg) were euthanized mid-afternoon with pentobarbital sodium (120 mg/kg), administered via a peripheral ear vein.

Preparation of tissues for microscopy

Immediately after euthanasia, neck blood vessels were severed and the animal laid on its side so the superior ocular cul-de-sac of one eye could be irrigated with 35^{o}C sterile saline and then fixative solution. The upper eyelid was then cut away and stretched to its extended configuration, palpebral surface uppermost, onto a thick cardboard support. A few drops of fixative solution ((2 % glutaraldehyde in 80 mM sodium cacodylate buffer, pH 7.2 to 7.4, 320 to 340 mOsm/kg), now at room temperature (RT), were applied every few minutes over a period of 2 h. The fixed eyelid was unpinned and placed in a vial of fixative at 4^{o}C until further processing for light microscopy (LM), scanning electron microscopy (SEM) or transmission electron microscopy (TEM).

Approximately one quarter (3 to 4 mm) of the lateral aspect of the eyelid was cut away and discarded. A narrow strip, approximately 1 mm in width, was then cut with a razor and the entire strip embedded in paraffin wax for light microscopy (LM) and stained with toluidine blue or haematoxylin and eosin. A second slightly narrower strip (0.5 to 1 mm) was then cut away and prepared for embedding in Araldite. For this, a tissue block including the most anterior edge of the eyelid (and approx. 2 mm in length) was cut and processed and examined essentially as previously detailed.[34] Overall, the goal was to obtain a few (5 to 10) acinar sections from each sample, cut at slightly different depths. A quite considerable proportion of the total number of sections viewed did not contain any acini or only a small part of one, and these were discarded. Thick sections were stained with toluidine blue, and then suitable thin sections stained with a lead citrate then uranyl acetate. A rectangular piece of the eyelid approximately 5 x 11 mm, was separately processed as previously detailed and examined by SEM.[30-32]

Morphometry

Measurements from images obtained by LM (at final magnifications of 40X and 100 X) were either evaluated using the line tool in Image Focus® (Euromex, Arnhem, Holland) or enlarged onto A3-sized prints (42 x 29.5 cm) and dimensional measurements then made with a rule to a final resolution of close to 1 μm (micron). From A3-sized prints, areas were measured with a digitizer pad (DigiPro, Elestree Computing, London) to 10 μm^2 (i.e. square microns) resolution. For TEM, a final magnification of between 1000X and 2000 X was selected so as to be able to generate a set of acinar profiles suitable for morphometry to include the full width (diameter) of the acinar unit (so that its overall size and area could be estimated) as well as allow for measurements of as many meibocytes as possible and their nuclei (while minimizing the change

of missing any extremely small nuclei). Some of these acinar measurements were simply made with the on-screen line tool, but most measures were made from A3-sized prints on pre-marked the cell borders and nuclei (see Figure 3B later). For the TEM images dimensional measures were made to approximately 0.2 μm resolution for dimensions and 0.05 μm^2 for areas. Measures of nucleus and cell areas were compared to assess the nucleo-cytoplasmic ratio, with the N/CELL area values being based on a (nucleus area / cell area) calculation.

Statistical analyses

All data were entered into spreadsheets in Systat for calculation of global statistics (mean ± SD) with normality of data sets being checked using the Shapiro-Wilk test, with a value of > 0.05 being considered normal. For comparisons between data sets, non-parametric rank order Friedman test was used, with a statistical difference being considered if $p = 0.05$ or less. Inter-dependence of morphological variables was undertaken to generate a Spearman correlation coefficient (r_s).

RESULTS

Low resolution LM of paraffin sections (Figure 1A) or Araldite embedded sections (Figure 1B) were selected so as to grossly sample the acinar units (lobules) adjacent to but not including the main anterior ductules, a sectioning perspective and view that has been presented by many other investigators as well.[6,9,11,12,15,16,18-20] Such sections showed clusters of lobules adjacent to the thickened conjunctival epithelium posterior to the oculo-mucocutaneous junction. The external aspect of a main duct can be seen just below the cluster of lobules (Figure 1A) for which the actual spatial positioning was variable, sometimes extending further towards the conjunctival epithelium.

The lobules (acini) were roundish in shape, often in apparent contact and appearing to be slightly overlapping. From a single representative example selected from several sections of each eyelid, between 12 and 19 lobule profiles were evident. The averaged dimensions of these lobule profiles ranged from 42 to 142 μm with a group mean (pooling data from all sections) of 86 ± 37 μm. The measured cross-sectional areas were between 1850 and 14900 μm^2, with a group mean area of 6155 ± 3934 μm^2 for the 6 eyelid samples. Little or no cellular detail was evident within the lobules, i.e. the borders of individual cells were rarely evident, but what appeared to cell nuclei of the meibocytes could be evident within some lobules.

A slightly higher magnification sagittal section of an Araldite-embedded sample (Figure 1B) illustrates how part of a Meibomian gland lobule could be close to the epithelial surface and just posterior to the thickest region of the conjunctival epithelium. As with wax sections, parts of lobules were usually evident with their edges in contact or even slightly overlapping in some locations and parts of them could now be seen to be composed of closely packed meibocyte cells. Most of these cells had rather prominently staining nuclei, and the cell-cell borders were usually evident. Measurements were made of the apparent longest dimension of individual lobules (but avoiding sections where the lobules appeared to be substantially overlapping) yielded a group mean of 94 ± 26 μm (range from 30 to 130 μm). Using these diameters to estimate lobule sectional areas approximating to a circular shape, yielded values from 707 to 13275 μm^2, for a group mean of 6941 ± 531 μm^2.

Within any particular lobule profile, between 30 and 75 meibocytes could be measured, with many having a slightly larger cross-sectional area than goblet cells that could be seen in the adjacent conjunctival epithelium in some sections (e.g. Figure 1B). The measured meibocyte cell area values were between 29 and 352 μm^2, with average values from any particular lobule being between 142 and 201 μm^2. For all sets of images, from 6 blocks processed from different eyelids, group mean of 179 ± 72 μm^2 was obtained for meibocyte

sectional area. Overall, when viewed from this sagittal perspective at low magnification, 62 % of the meibocytes appeared to have a prominently-staining nucleus, although very small nucleus profiles would not have been resolved. Whether in individual lobules, or if all data were considered, no measurable differences in meibocyte area values were detected according to whether or not a nucleus was obviously present in these cells ($p \geq 0.2$).

Figure 1C shows the appearance of the palpebral surface at the anterior location as viewed by SEM at low magnification (100 X), with the image oriented to align with the LM imaging. At the lower portion of Figure 1C can be seen some exfoliated cells while above this zone can be seen three dark round to slightly oval 'blobs' of the extruded meibum. Distal to these orifices, the eyelid marginal zone was seen to be relatively smooth but with two distinctive lines across it. About 0.2 to 0.3 mm distal to the gland orifices can be seen a ridge or crease (see single arrowhead), while a little further across the surface was another slightly more accentuated ridge (see double arrowheads) with some exfoliating cells just visible. This narrow zone, approximately 0.2 mm wide, is considered to be the oculo-mucocutaneous junction. In studies on separate rabbits, this can be seen to 'stain' weakly with lissamine green with no obvious staining either side of it. Beyond this narrow zone, at the top of the image, a range of light to dark electron reflexes of surface cells was routinely visible across the palpebral (tarsal) surface.

In contrast to the sagittal sections, coronal sections of Araldite-embedded eyelid tissue routinely revealed lobules as individual units clearly separated from each other by connective tissue, with no overlap. The various features and different aspects of the acinar structures that were seen in coronal section imaged by TEM are illustrated in Figures 2 to 4. The acini had two distinct appearances. In Figure 2A is shown a sectional profile through a small acinus surrounded by collagen fibril bundles and some fibroblast-like cells. The individual meibocytes and their nuclei are clearly resolved and of similar size. The cytoplasm contains variable numbers of non-staining (translucent) circular features which are the oil droplets. In peripheral (edge) locations are elongated cells with few oil droplets in them and these are assumed to be largely undifferentiated or immature basal meibocytes. There are also some partly differentiated meibocytes just in from the edges (with quite a high number of oil droplets in their cytoplasm) and also more centrally-located mature meibocytes (with large numbers of oil droplets in their cytoplasm). Figure 2B shows where almost the entire acinar content was transformed into an amorphous emulsion with almost no signs of individual cells being evident. This hypermature lobule is surrounded by ductule epithelium beyond which are small collagen fibril bundles. That the contents of acinar unit are transformed from the meibocytes is indicated by the spheroid-like profile of the largely emulsified contents, especially towards the upper left hand side, and that at the extreme left hand side are the remnants of individual cells. These cells still have visible nuclei, the sizes of which are very similar to those in the adjacent mature (non-transformed) acinar unit where the individual meibocytes are still intact. Even larger acinar profiles were encountered, with an image of part of one of these being shown Figure 3A, where there are some smaller peripheral (edge) cells (with few oil droplets) but also some much larger differentiated cells (with large numbers of oil droplets) immediately adjacent to these basal cells. In other examples (Figure 4), peripherally-located (edge) meibocytes were differentiated with very prominent oil droplets. The collagen bundles surrounding the acinar unit are also evident in Figure 3A, and two slightly higher magnification images from different acini are shown in Figure 4 to better illustrate these collagen bundles. A rather thin and irregular basement membrane can just be discerned at the outer edges of peripheral meibocytes in Figure 4.

In some meibocytes, the nucleus profiles were slightly elongated (oval) while others appear more rounded. Some meibocyte nuclei towards the periphery tended to have smoother

edge profiles compared to those towards the center (Figure 2A, Figure 4) but other more peripheral meibocytes did not have elongated nuclear profiles (Figure 3A, Figure 4). A smaller nucleus profile, with a slight indentation, can also be seen in the center of Figure 4B. Distinct crenations to the profiles were sometimes evident. In addition, a few cells appeared to have more than one nucleus included in what appeared to be the profile of the cells, with one of these nucleus profiles perhaps being somewhat smaller.

Small elongated (flattened) bundles of collagen fibrils were a consistent feature in close proximity to the intact acini. In Figure 4A, for example, the sets of bundles were approximately 7 μm in length and 1.5 μm thick. From fourteen other similar micrographs the average values for bundle length were between 5 and 8 μm, with thickness values between 1.2 and 1.7 μm. There were between 3 and 7 bundles, essentially lying side by side around the edges of the acini, sometimes interspersed with fibroblast-like cells.

In undertaking detailed morphometry, the overall size and cellular features were assessed for all acini, and then the cellular details were considered in relation to the location of the meibocytes within the acini and their presumed maturity. The maturity was largely based on the content of oil droplets. For the meibocytes in Figure 2A, the density of the oil droplets ranged from relatively sparse (see right hand side of Figure 2A), to moderate (see left hand side of Figure 2A) to substantial (see middle and lower portion of Figure 2A). In Figure 3A, most of the peripheral meibocytes had low numbers of small oil droplets while most of those located towards the center had greater numbers of larger oil droplets. However, as shown in Figure 4 even the most peripheral (EDGE) meibocytes could contain large numbers of lipid droplets.

Overall, the acini could be small (e.g. Figure 2A, where the estimated diameter is close to 35 μm) or much larger (Figure 3A, diameter close to 70 μm). Diameter measurements of intact acini, taken from a total of 86 different images from multiple Araldite sections from each of the 6 tissue blocks yielded an overall group mean of 82 ± 17 μm (range 31 to 111 μm). Using the larger dimensional value to calculate a cross-sectional area estimate, yielded areas between 707 and 9853 μm^2 in area, for a group mean of 5542 ± 1154 μm^2. By way of contrast, for the transformed acinus shown in Figure 2B, the longest dimension was estimated to be 105 μm, and similar sizes (range 96 to 139 μm, mean 117 ± 37 μm) were found in 22 other images, 17 of which appeared to be completely transformed and surrounded only by ductule epithelium (rather than flattened collagen bundles). Rather than being considered as acinar sizes, these latter measures could also indicate the diameter of the ductules.

Within the acini, the sizes of individual meibocytes were assessed by marking the cells and their nuclei on the prints (see Figure 3B). Overall, from any particular (part) sectional view of an acinus, between 4 and 17 meibocytes were measured across 47 different sections, with 83 % of the cells including a nucleus (see later). As assessed in all meibocytes regardless of nucleus status, cell area values ranged from 58 to 381 μm^2, with a group mean of 158 ± 81 μm^2 (median 148 μm^2). The cells were then subjectively categorized according to location (Figure 5A) and maturity (Figure 5B). For meibocytes located in the central (CENTER) regions of the acini, the mean sectional area was 168 ± 97 μm^2 (median 145 μm^2), while for those in the more peripheral edge (EDGE) regions of the acini the averaged data indicated a trend to smaller cells (mean of 149 ± 67 μm^2) but not significant ($p = 0.730$). In contrast, the immature meibocytes (based on having less than 25 oil droplets) were smaller in size (mean area of 105 ± 37 μm^2; median 108 μm^2) as compared to mature cells (mean area 206 ± 81 μm^2; median 206 μm^2); the difference was significant ($p < 0.001$).

For meibocytes that appeared to have just a single nucleus, the nucleus area profiles ranged from 5 to 52 μm^2, for a group mean of 29.4 ± 11.7 μm^2, with these nucleated cells having a mean sectional area of 167 ± 87 μm^2. Essentially the same wide range of nucleus area values were encountered at both CENTER and EDGE locations with little difference in

both averaged values (Table 1) and median values (Figure 6A); no difference was detectable ($p = 0.730$). The same also applied when the meibocytes were categorized according to maturity (Figure 6B), again with no differences in nucleus size being detectable ($p = 0.982$) (Table 1).

The calculated N/CELL area ratio values ranged from 0.024 to 0.544, for a group mean of 0.219 ± 0.131 (median 0.188). When considering all cells, correlation analyses indicated the smaller ones had higher N/CELL area values while those in larger cells were lower ($p = 0.002$, $r_s = - 0.604$). The N/CELL area ratios were found to be different according to location (Figure 7A) and maturity (Figure 7B). For peripherally-located (EDGE) meibocytes, the nuclei generally occupied a larger proportion of the cell section and so higher N/CELL area ratios were encountered (Table 1); the difference, however, just failed to reach statistical significance ($p = 0.080$). However, when categorized by the extent of differentiation (IMMATURE vs. MATURE), the more peripheral (and immature) cells had distinctly higher N/CELL area ratio values, while the more centrally-located (and more mature) meibocytes had lower N/CELL area ratios ($p = 0.002$) (Figure 7B, Table 1).

DISCUSSION

The present studies provide basic data on the Meibomian gland acini that has not been reported previously, and indicate that better sectioning and viewing methods (as well as objective assessments) are needed to underpin histopathological diagnoses of gland dysfunction. For example, the differences in cell size and their nucleo-cytoplasmic (N/C) features indicate distinct maturation-related differences. The N/C aspects of the cells also indicate that the meibocyte transformation does not obviously occur by 'degeneration' (at least in rabbits), but rather by a simple lytic process associated with a critical level of oil droplets in the cells. That there are now some measured characteristics of the Meibomian gland acini, as well as on acinar size, should provide a useful and necessary basis for development of objective assessments of Meibomian gland dysfunction (MGD), including in any animal dry eye models, especially since even medical treatment of MGD is a largely empirical undertaking.[29]

The special fixation methods were undertaken to minimize the chance of substantial measurement artefacts. For example, the surface of the eyelid marginal zone was relatively smooth in extended state and did not show numerous substantial creases or 'rugae'.[35] While the macroscopic appearance of the gland may well be considered to be acceptable in eyelid tissue that is not stretched out before fixation, details of the gross organization, fine structure and ultrastructure could be substantially different when sections are made from eyelid pieces that were simply cut out and placed in fixative solutions.

The main choice of coronal sections for this study makes it different from most previous protocols because the anterior portion of the eyelid can include sectional portions of the Meibomian glands in what might be referred to as oblique, glancing, skewed or para-sagittal sections. This is where parts of both coronal and sagittal perspectives of the acini are visible in the same tissue section. Tissue sections with a dominant sagittal (longitudinal) perspective are those that have been more commonly obtained and presented. This has not obviously been considered previously, especially in terms of the interpretation of the images seen.[1,3,4,10,14,24] The organization of the acini in sagittal sections was not found to be suitable for objective assessments especially because there was no obvious organization into smaller peripheral (basal) cells versus larger centrally-located differentiated cells. Such differences can be partially apparent in an oblique section,[4] and the same conclusion can be drawn from similar (para)sagittal sections through the acini.[9,23,24,26] Tritium labeling,[25] or BrdU labeling,[28] can be undertaken to identify basal cells predominantly in the periphery of the acini, and morphometry could perhaps be undertaken on these labeled cells Notwithstanding, a useful morphometric

index, even off sagittal sections, might be the apparent number of meibocytes in any particular lobule and for which an approximate value of between 35 and 40 would seem reasonable for rabbit acini. This could facilitate distinguishing normal ranges of cell sizes from abnormal, or what was referred to as squamous metaplasia of the alveolar cells of the glands.[11]

The coronal perspective of the acini has sometimes been seen by chance in sections from human tissue, [8,10,14] and this is essential to show that peripherally-located (edge) meibocytes (that are more likely to include the 'basal' or immature cells) tended to be smaller, have higher nucleo-cytoplasmic area ratios but few oil droplets. In contrast, more centrally located meibocytes tended to be slightly larger, had lower or much lower nucleo-cytoplasmic ratios and many oil droplets. In agreement with a previous note,[24] the N/C ratios of immature (basal) cells can be 'high', averaging around 0.3, but greater N/C ratios might be found at deeper locations in the glands where 'immature' acini are presumably located.

Subjective examination of histology sections (that include parts of the Meibomian glands) will likely reveal some meibocytes to be obviously nucleated while others appear to have lost their nuclei.[4,10,23,24] It has been implied that this is a specific process that occurs in acini that are close to secretory ductules,[23] and the same concept is presented in a later study.[4] It has also been noted that the nuclei can become distorted and disappear,[10] or that they can have an irregular profile.[14] A distortion of the nucleus profile could be sign of crenation associated with a progressive shrinkage, and so a possible transition between these two extremes (of nucleated and non-nucleated) could be that some nuclei appear to be substantially reduced in size; this process may be referred to as pyknosis.[4] In mature acini, therefore, if such a nuclear change is specifically related to the transformation of the meibocytes into meibum, a distinct set of cells with pyknotic nuclei might be expected, but no obvious sub-population of shrunken (very small) nuclei were observed. Indeed, the meibocyte nuclei do not have to be substantially altered in size in relation to the acinar location or impending transformation (Figure 2B). More specific evaluation of nucleus size and shape profile is needed to assess whether predictable changes occur in relation to meibocyte maturation.

An acinar profile that seemed to be of just immature meibocytes with no or only very few oil droplets was not encountered in the tissue blocks used in the present studies, or in several other blocks taken from unstretched or partially stretched eyelid specimens not included in the present study. Such a structure been has not been reported in other publications that could be located. It could be that immature acini are only found further back along the gland, even though saggital sections through the glands do not indicate obvious differences in the lobules along the length of the glands.[1-4,14,16,18,23,24,36]

In addition to not seeing immature acini, no partially transformed acini were seen, i.e. an acinar unit with perhaps half the meibocytes having disintegrated. Completely intact acini (with cells in various stages of maturation) can be found in very close proximity to fully transformed acinar units [e.g. Figure 2B and also Figure 1,[29]]. It has been noted that there can be differences in lipid or alkaline phosphatase enzyme staining between the periphery and center of alveoli.[7] It was expected that at least some of the acini would have a structural organization indicative of partial trasformation, even though such a structure has not obviously been reported by other investigators either. Finding such acini will be useful to answer questions related to the kinetics of meibocyte disintegration and thus the basic functioning of these secretory units.

In conclusion, acinar cells of the rabbit Meibomian glands, especially if viewed in coronal sections, can be objectively assessed with a range of simple morphometric measures. The overall size of the acinar lobules appears to be reasonably predictable and (at least from a macroscopic perspective) apparent length and width measurements can be made as a possible basis for assessing whether or not acini are abnormal, in being either distended or atrophic. Consideration of meibocyte density, the size and nucelo-cytoplasmic ratios of these cells should

also be useful indicators to assess how factors such as age and inflammation might alter these glands.

REFERENCES

1. Prince JH, Diesem CD, Eglitis I, Ruskell GL. The Anatomy of the Eye and Orbit in Domestic Animals. Charles C. Thomas, Springfield; 1960, pp. 47 and 278.
2. Samuleson DA. Ophthalmic anatomy. In – Veterinary Ophthalmology (ed. Gelatt KN). 4th edn, volume 1, 2007; pp. 42-46.
3. Oyster CW. The eyelids and the lacrimal system. In – The Human Eye. Sinauer Associates, Philadelphia, 1999; pp. 293.
4. Knop N, Knop E. Meibom-Drüsen. Teil 1: Anatomie, Embryologie und Histologie der Meibom-Drüsen. *Ophthalmologe* 2009; 106: 872-883.
5. Wolfram-Gabell R, Sick H. Microvascularization of the mucocutaneous junction of the eyelid in fetuses and neonates. *Surgigcal Radiology Anatomy* 2002; **24**: 97-101.
6. Milz S, Neufang J, Higashiyama I, *et al.* An immunohistochemical study of the extracellular matrix of the tarsal plate in the upper eyelid of human beings. *Journal of Anatomy* 2005; **206**: 37-45.
7. Rondinini R. Ricerche istochimiche sulla ghiandola del Meibomio nei mammiferi. *Bullettino Scienze Mediche (Bologna)* 1955; **127(4)**: 323-334.
8. Seifert P, Spitznas M. Immunocytochemical and ultrastructural evaluation of the distribution of nervous tissue and neuropeptides in the meiboian gland. *Graefe's Archives Clinical Experimental Ophthalmology* 1996; **234**: 648-656.
9. Stephens LC, Schulttheiss TE, Vargas KJ, *et al.* Glands of the eyelids of Rhesus monkeys (Macaca mulatta). *Journal Medical Primatology* 1989; 18: 383-396.
10. Weingeist TA. The glands of the ocular aneexa. In – Ocular Fine Structure for the Clinician (ed. Zinn KM). *International Ophthalmology Clinics* 1973; **13(3)**: 243-261.
11. Kohno T, Ohnishi Y. Histopathology of Meibomian gland abnormalities in experimental PenCB intoxiciated beagle treated with squalene [In Japanese]. *Fukuoka Igaka Zasshi* 1989; **80**: 258-262.
12. Baba MA, Sinha R, Prasad R, Prasad J. Comparative histological and histochemical studies on the Meibomian glands of goat and sheep. *Indian Journal Animal Science* 1990; **60**: 1085-1087.
13. LeDoux MS, Zhou Q, Murphy RB, *et al.* Parasympathetic innervation of the Meibomian glands in rats. *Investigative Ophthalmology Visual Sciences* 2001; **42**: 2434-2441.
14. Obata H. Anatomy and histopathology of human Meibomian gland. *Cornea* 2002; **21 (suppl. 2)**: S70-S74.
15. Kozak I, Bron AJ, Kucharova K, *et al*. Morphological and volumetric studies of the Meibomian glands in elderly human eyelids. *Cornea* 2007; **26**: 610-614.
16. Mauris J, Dieckow J, Schob S, *et al.* Loss of CD147 results in impaired epithelial cell differentiation and malformation of the meibonian gland. *Cell Death Disease* 2015; **6**: e1726.
17. Ohnishi Y, Kohno T. Polychlorinated biphenyls poisoning in monkey eye. *Investigative Ophthalmology Visual Sciences* 1979; **18**: 981-983.
18. Obata H, Horiuchi H, Miyata K, *et al.* Histopathological study of the Meibomian glands in 72 autopsy cases [In Japanese]. *Acta Societas Opthalmologica Japonica* 1994; **98**: 765-771.
19. Perra MT, Serra A, Sirigu P, Turno F. Histochemical demonstration of acetylcholinesterase activity in human Meibomian glands. *European Journal Histochemistry* 1996; **40**: 39-44.
20. Nien CJ, Paugh JR, Massei S, *et al.* Age-related changes in the meibomian gland. *Experimental Eye Research* 2009; **89**: 1021-1027.
21. Ibrahim OMA, Dogru M, Matsumoto Y, *et al.* Oxidative stress induced age dependent Meibomian gland dysfunction in Cu,Zn-superoxide dismutase-1 (Sod1) knockout mice. *PLOS One* 2014; **9**: e99328.

22. Suhalim JL, Parfitt GJ, Xie Y, *et al.* Effect of desiccating stress on mouse Meibomian gland function. *Ocular Surface* 2014; **12**: 59-68.
23. Miraglia T, Gomes NF. The Meibomian glands of the marmoset (Callithrix jacchus). *Acta Anatomica* 1969; **74**: 104-113.
24. Jester JV, Nicolaides N, Smith RE. Meibomian gland studies: histologic and ultrastructural investigations. *Investigative Ophthalmology* 1981; **20**: 537-547.
25. Olami Y, Zajicek G, Cogan M, *et al.* Turnover and migration of Meibomian gland cells in rats' eyelids. *Ophthalmic Research* 2001; **33**: 170-175.
26. Cheriyan T, Schmid TM, Spector M. Presence and distribution of the lubricating protein, lubricin, in the Meibomian gland in rabbits. *Molecular Vision* 2011;**17**: 3055-3061.
27. Nien CJ, Massei S, Lin G, *et al.* Effects of age and dysfunction on human Meibonian glands. *Archives Ophthalmology* 2011; **129**: 462-469.
28. Beyazyildiz E, Pinarli FA, Beyazyildiz O, *et al.* Efficacy of topical mesenchymal stem cell therapy in the treatment of experimental dry eye syndrome model. *Stem Cells International* 2014; article ID 250230.
29. Doughty MJ. On the prescribing of oral doxycycline or minocycline by UK optometrists as part of management of chronic Meibomian Gland Dysfunction (MGD). *Contact Lens Anterior Eye* 2016; **39**: 2-8.
30. Doughty MJ. Scanning electron microscopy study of the tarsal and orbital conjunctival surfaces compared to peripheral corneal epithelium in pigmented rabbits. *Documenta Ophthalmologica* 1997; **93**: 345-371.
31. Doughty MJ. Normal features of superficial non-desquamating cells of the rabbit corneal epithelium assessed by scanning electron microscopy. *Veterinary Ophthalmology* 2008; **11**: 81-90.
32. Doughty MJ. Functional morphology of mucosal goblet cells based on spatial separation of orifice openings to the surface – application of the rabbit bulbar conjunctiva. *Tissue Cell* 2014; **46**: 241-248.
33. Doughty MJ. A systematic assessment of goblet cell sampling of the bulbar conjunctiva by impression cytology. *Experimental Eye Research* 2015a; **136**: 16-28.
34. Doughty MJ. Assessment of size and nucleo-cytoplasmic characteristics of the squamous cells of the corneal epithelium. *Clinical Experimental Optometry* 2015b; **98**: 218-223..
35. Pfister RR, Renner ME. The corneal and conjunctival surface in vitamin A deficiency – a scanning electron microscope study. *Investigative Ophthalmology Visual Science* 1978; **17**: 874-883.
36. Linton RG, Curnow DH, Riley WJ. The Meibomian glands. An investigation into the secretion and some aspects of the physiology. *British Journal Ophthalmology* 1961; **45**: 718-723.

TABLE 1

MORPHOMETRY OF MEIBOCYTES AND THEIR NUCLEI IN ANTERIOR PORTION OF RABBIT MEIBOMIAN GLANDS

	LOCATION of MEIBOCYTES in ACINI	
	EDGE	CENTER
CELL SECTIONAL AREA (μm^2)	168 ± 97	149 ± 67
NUCLEUS SECTIONAL AREA (μm^2)	29 ± 11	31 ± 13
N/CELL AREA RATIO	0.244 ± 0.202	0.157 ± 0.111
	MATURITY of MEIBOCYTES	
	IMMATURE	MATURE
CELL SECTIONAL AREA (μm^2)	105 ± 37	206 ± 81
NUCLEUS SECTIONAL AREA (μm^2)	29 ± 10	30 ± 14
N/CELL AREA RATIO	0.309 ± 0.121	0.128 ± 0.050

All values mean ± SD.

Figure captions

Figure 1 Eyelid marginal zone seen in paraffin sections (A) to illustrate lobules of the Meibomian glands (marked MG), in thick sections from Araldite-embedded tissue (B) showing part of a lobule of the gland (also marked (MG) that can be seen to contain numerous meibocytes, and (C) scanning electron microscopy to show the surface of the marginal zone. In (B), the location of the MG lobule in close proximity to the thickened region of the conjunctival epithelium should be noted, the distal regions of which include some goblet cells (marked GC). In (C) the single and double arrowheads indicate the approximate location of the anterior and posterior boundaries of the oculo-mucocutaneous junction respectively. Scale bars indicate 0.15 mm, 0.05 mm and 0.2 mm respectively.

Figure 2. Lower magnification transmission electron microscopy (TEM) images to illustrate (A) a coronal section through a small partly-differentiated acinar unit with distinct cells (meibocytes) visible in the acini and (B) an almost fully transformed much larger lobule adjacent to a ductule to show the emulsification of the acinar contents. Scale bar = 7 μm in (A) and 22 μm in (B).

Figure 3. Lower magnification transmission electron microscopy (TEM) image to illustrate (A) coronal section through part of larger partly-differentiated acininus with distinct cells (meibocytes) visible in the acini, and (B) the marked print showing the cell domains and their nuclei. Scale bar = 14 μm.

Figure 4. Slightly higher magnification transmission electron microscopy (TEM) images to illustrate coronal sections through peripheral regions of larger partly differentiated acini with distinct cells (Meibocytes) visible in the acini and the collagen bundles that surround the periphery of the acini. Bar = 7 μm in (A) and 5.5 μm in (B).

Figure 5. Meibocyte sizing according to location (CENTER versus EDGE) (A) or apparent maturity (IMMATURE versus MATURE) (B). Cell sectional area values in μm^2. Data from 46 sections from 6 tissue blocks.

Figure 6. Box plots to illustrate differences in nucleus area profiles according to location (A) and maturity (B) of meibocytes. Nucleus sectional area values in μm^2.

Figure 7. Box plots to illustrate differences in nucleus-to-cytoplasmic ratios according to location (A) and maturity (B) of meibocytes.

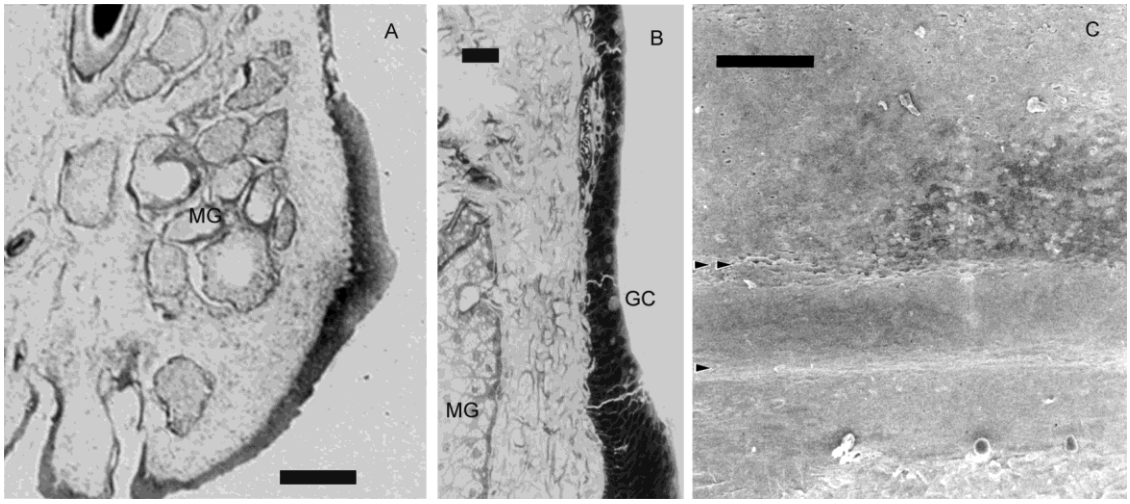

FIGURE 1

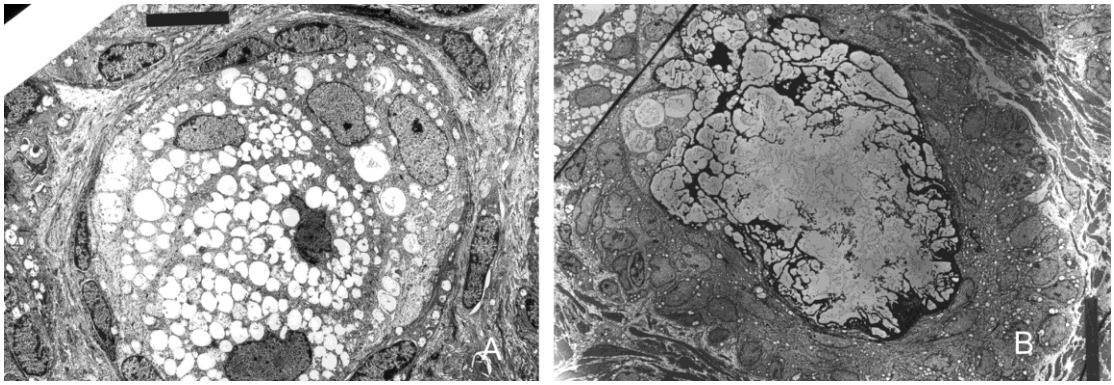

FIGURE 2

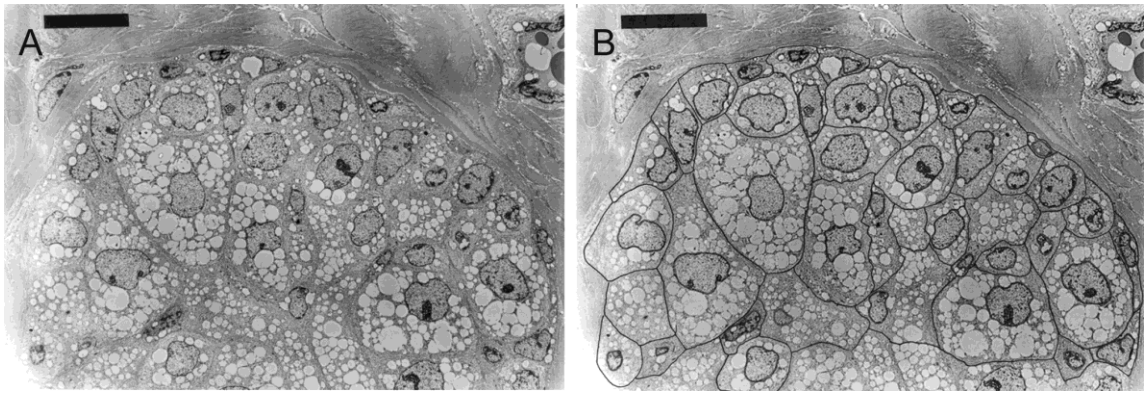

FIGURE 3

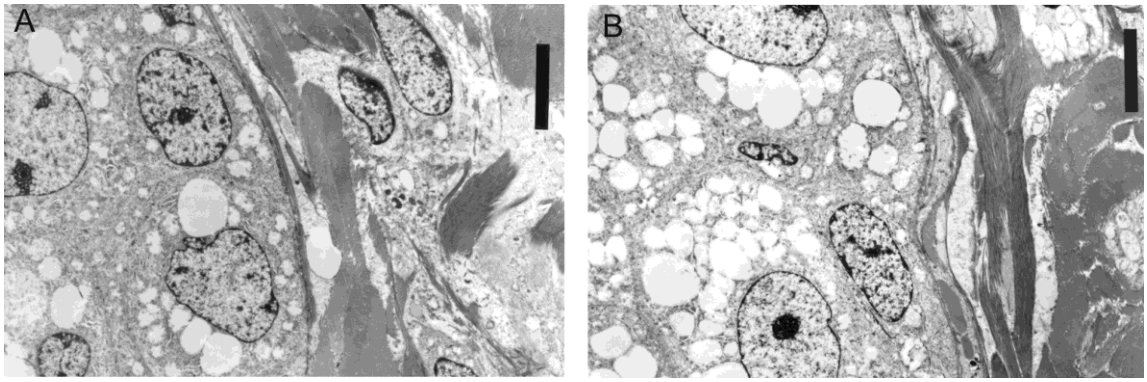

FIGURE 4

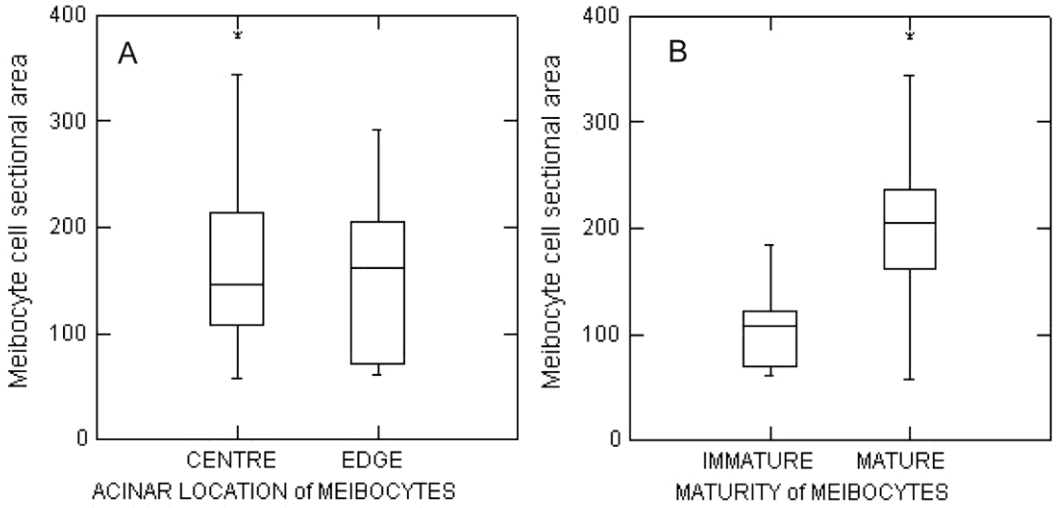

FIGURE 5

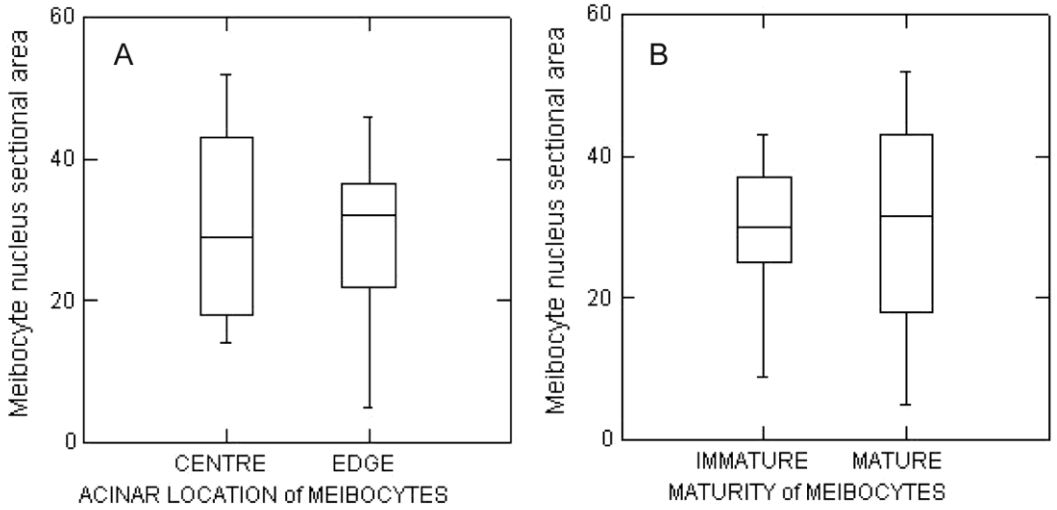

FIGURE 6

I

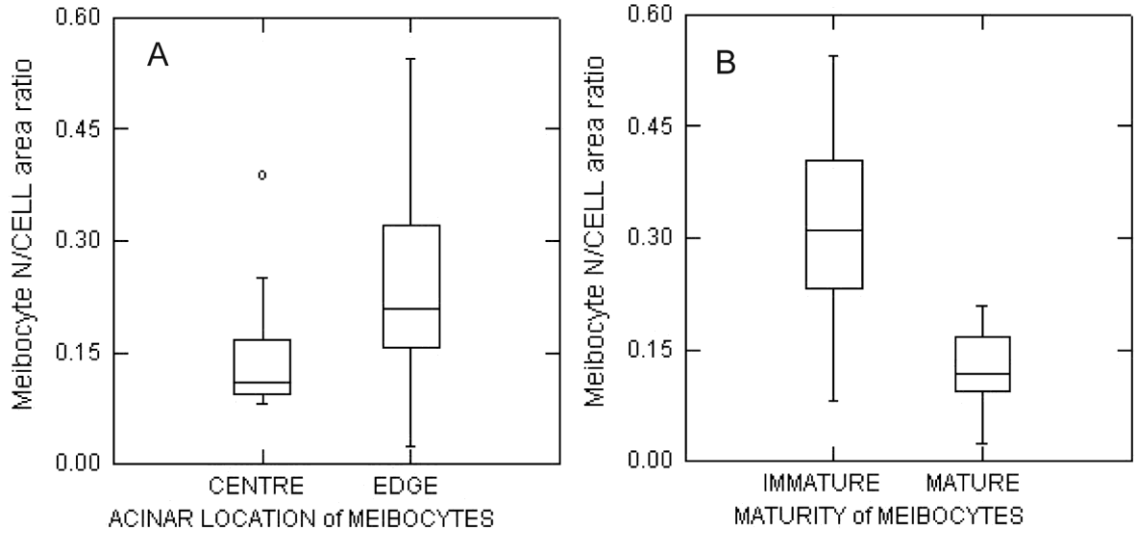

FIGURE 7